Numerical Reproducibility of Human Body Model Crash Simulations

Citation for the original published paper (version of record):

Östh, J., Pipkorn, B., Forsberg, J. et al (2021). Numerical Reproducibility of Human Body Model Crash Simulations. Conference proceedings International Research Council on the Biomechanics of Injury, IRCOBI: 431-443

Numerical Reproducibility of Human Body Model Crash Simulations

Jonas Östh, Bengt Pipkorn, Jimmy Forsberg, Johan Iraeus

Abstract The numerical reproducibility of a Finite Element (FE) Human Body Model (HBM) was evaluated by quantifying the variation in model predictions for diverse computer systems at different sites and settings. Repeated simulations, with varying number of Central Processing Unit (CPU) cores and model decomposition, of four high severity load cases – a full frontal, near-side frontal oblique and side impact with a full set of driver restraints, as well as a full frontal with a seat belt only restraint – was carried out on five computer systems. HBM responses were found to vary randomly with the Number of CPU cores (NCPU), but not due to different hardware or message parsing interface software at each computer system used. Implemented HBM updates reduced the variation in the near-side frontal oblique load case. When the NCPU used was fixed, identical results were obtained from all computer systems. This means the variation of HBM responses is due to the model decomposition. It is possible to quantify the numerical reproducibility of an FE HBM by repeated simulations, varying the NCPU and analyzing the coefficient of variation of the responses.

Keywords Reproducibility, Human Body Model, Finite Element, Virtual Testing

I. INTRODUCTION

Repeatability and reproducibility of physical Anthropomorphic Test Devices (ATDs) has been studied extensively. Foster *et al*. [1], for instance, showed a repeatability Coefficient of Variation (CV) for repeated Hybrid III tests of approximately 5% and improved reproducibility in comparison with the Hybrid II. The rear-end impact response of the BioRID II and RID2 ATDs has been scrutinized, and better repeatability and reproducibility of the RID2 was found [2]. Furthermore, a repeatability and reproducibility study of the thorax response of the THOR ATD compared to that of the Hybrid III showed that there was a higher CV for THOR [3].

The rating organization Euro NCAP plans to introduce virtual testing, using Finite Element (FE) Human Body Models (HBMs), in the rating protocol [4–5]. This means that assessing repeatability and reproducibility of HBM simulations will also be necessary. Repeatability and reproducibility, are slightly different for FE HBMs, however, compared to physical human surrogates, such as ATDs. Theoretically, neither repeatability nor reproducibility should be of any concern for a numerical model, as long as the underlying partial differential equations can be solved accurately. But this is most often not possible in real life applications, except for very simple numerical models. Applied impact biomechanics models, such as FE HBMs used for vehicle safety simulations, must be solved using numerical approximations. Thus, the results will be more or less dependent on the settings controlling the approximations and the numerical precision of the computer system used. In addition, state-of-the-art vehicle safety FE simulation models are so large that they cannot be efficiently solved on a single Central Processing Unit (CPU). Instead, the FE simulation model is decomposed to several CPUs and solved using Message Parsing Interface (MPI) technology for CPU-to-CPU communication. Numerical repeatability, defined here as the running the same model (including all solver settings) on the same CPUs with the same MPI settings, is expected to be perfect and to give the same results all the time. Numerical reproducibility, defined here as running the same model on a different computer system using different MPI settings but with the same solver settings, could, on the other hand, give a variation in results due to differences in the solution introduced by hardware or software differences. The aim of this study is to quantify the variation in simulation results caused by solving with different computer systems and decompositions, using a state-of-the-art FE HBM.

J. Östh, PhD (e-mail: jonas.osth@volvocars.com, +46 728 88 91 72), is a Safety Analysis CAE engineer at the Volvo Cars Safety Centre, Gothenburg, Sweden. B. Pipkorn, PhD, is Director of Simulation and Active Structures at Autoliv Research, Vårgårda, Sweden. J. Forsberg, PhD, is Support Manager at Dynamore Nordic AB, Linköping, Sweden. J. Iraeus, PhD, is a Senior Researcher, J. Östh is an Adjunct Associate Professor, B. Pipkorn an Adjunct Professor at Chalmers University of Technology, Sweden. All authors are associated with SAFER – Vehicle and Traffic Safety Centre at Chalmers in Sweden.

II. METHODS

The SAFER FE HBM represents a 50th percentile male (175 cm, 77 kg [6]) occupant and was originally based on the THUMS v3, but as of the v10 update [7] most parts have been updated or replaced. Specific model updates include an updated KTH head model [8], a rib cage with statistically based 50th percentile male shape [9], updated cervical and lumbar spines [10], a statistically based 50th percentile male pelvis and updated subcutaneous soft tissues [7]. The model has an active muscle package utilizing feedback control to model human postural control [11–12] in the pre-crash phase. The FE simulations were made with the explicit Finite Element (FE) solver LS-DYNA MPP R9.3.1 Single Precision (LSTC, Livermore, CA).

SAFER HBM v10 Updates in Order to Improve Numerical Reproducibility

The previous SAFER HBM v9 had in total 160 contacts, which were reduced to 43 in SAFER HBM v10 [7]. The purpose of this change was to improve computational efficiency and reproducibility in distributed simulations, by the decomposition of a few large contact definitions rather than many small ones. Surface-to-surface contacts were replaced, as far as possible, by one general single-surface contact covering the axial skeleton, the thoracic and abdominal cavities and the proximal part of the extremities (Fig. 1(a)). For the distal extremities, four individual single-surface contacts were created and in addition some specialized surface-to-surface contacts were introduced, for instance in the knee area. For all these contacts a segment-based contact algorithm (LS-DYNA contact option SOFT=2) was used, together with a static and dynamic friction (FS=FD=0.1) for contacts inside the body, and 20% viscous contact damping (VDC=20). Both friction and damping were included to reduce numerical noise from the contact. All segment-based contacts were ensured to be free from initial intersections and penetrations. Tied contacts were used to connect the extremities to the soft tissue mesh, and a sliding only contact was used as a boundary condition between the brain and skull. Compared with the v9, this sliding only contact was updated to AUTOMATIC_SURFACE_TO_SURFACE_TIEBREAK contact with OPTION=4. As another step to reduce the numerical noise of the model, all parts modelled with elastic materials (*MAT_ELASTIC) in the model (Fig. 1(b)) were assigned a stiffness-based Rayleigh damping of 5% (*DAMPING_PART_STIFFNESS, COEFF=0.05) to reduce high frequency oscillations.

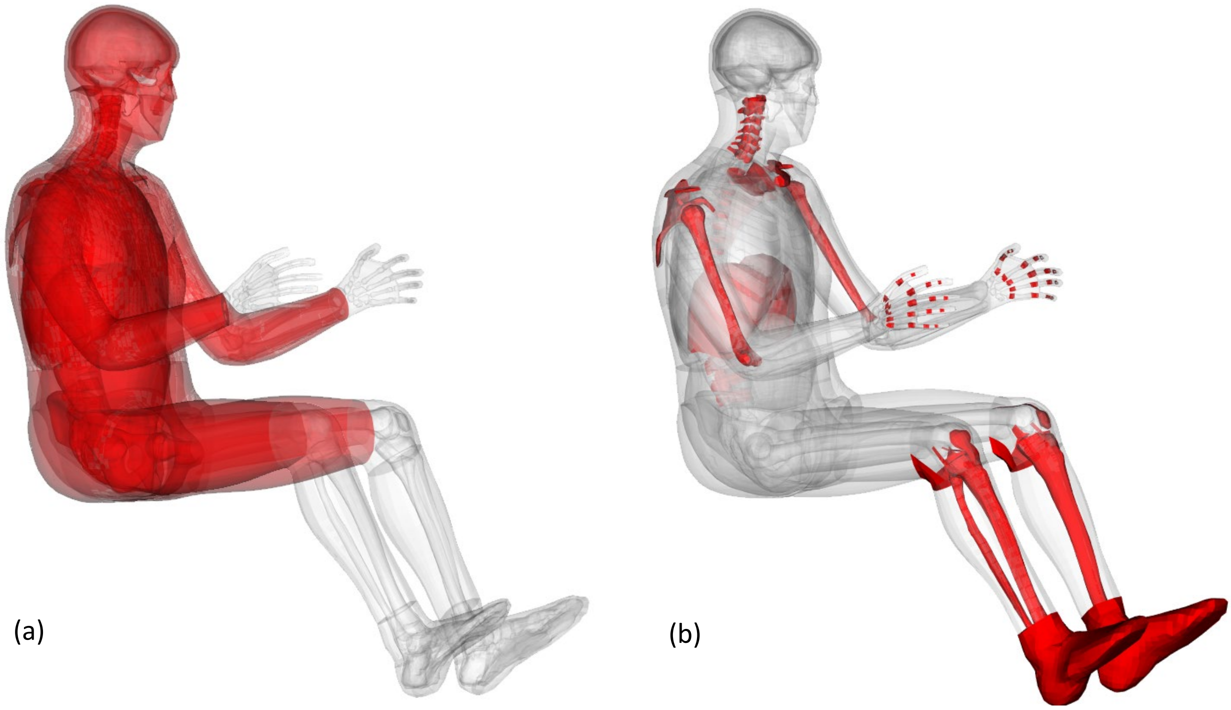

Fig. 1. SAFER HBM v10 updates to improve numerical reproducibility. (a) Several contacts were grouped into one general single-surface, segment-based contact, shown in red. (b) Parts with elastic only material model in the SAFER HBM v10 with added *PART_DAMPING_STIFFNESS of 0.05 highlighted in red.

Numerical Reproducibility Study

To evaluate the numerical reproducibility of the SAFER HBM v10 and to evaluate the effect of the model updates compared with the previous v9 [13], simulations with a generic vehicle sled model [14] were conducted on five distributed High Performance Computer (HPC) systems (one at Volvo Cars (VC), three different systems at Autoliv Research (ALR1–3), and one at Chalmers University (CU)). On the VC computer system Intel Xeon E5-2690 v4 CPUs and Platform MPI 9.1.4.3 were used. For ALR1 Intel Xeon E5-2667 v4, ALR2 Xeon E5-2667 v3, and ALR3 Xeon E5-2670 CPUs were used together with Platform MPI v8.1.1. The CU computer system consisted of Intel Xeon Gold 6130 CPUs and Intel MPI 2018b MPI software.

Four high severity load cases (Fig. 2), designed to test the numerical robustness of the HBM, were run: full frontal (FF); near-side frontal oblique (OBL) in driver position with a pre-tensioned, 4.2 kN load-limited seat belt and steering wheel-mounted airbag; a near-side impact (SIDE) with and additional seat mounted side airbag, and inflatable curtain (IC); and lastly a "rear seat" full frontal impact (FFR) with a pre-tensioned 6 kN load-limited seat belt (the same seat was used, but contact with the instrument panel was removed). For the FF and FFR load cases the change in velocity (ΔV) was 70 km/h and peak acceleration 38.2 g, while for the OBL load case the ΔV was 65 km/h and the peak acceleration was 24.7 g at a pulse angle of 29° from the longitudinal. For the SIDE load case the ΔV was 32 km/h and 310 mm lateral intrusion at a peak velocity of 13 m/s was included. These load cases were selected as they represent a large portion of applicable loading conditions for an occupant HBM.

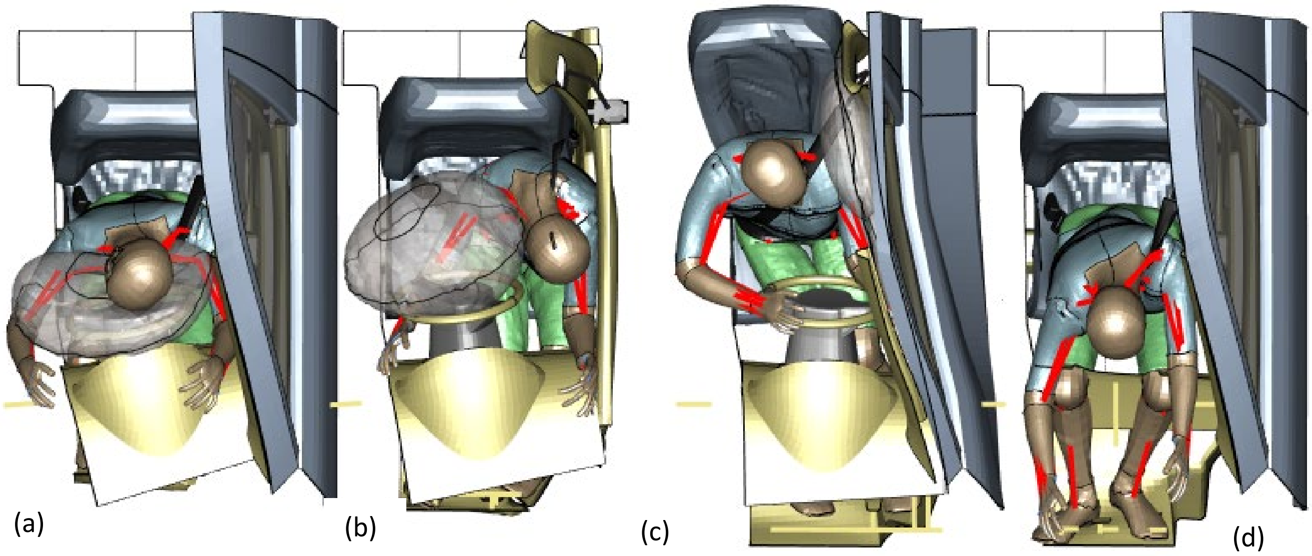

Fig. 2. (a) Full frontal (FF) crash simulation. (b) Near-side frontal oblique (OBL) simulation. Model slides off steering wheel-mounted airbag. (c) Near-side (SIDE) impact simulation with intruding structures and IC. (d) Rear seat full frontal (FFR) impact simulation without instrument panel.

For the SAFER HBM v10 in the FF load case, six repeated simulations were made at VC, ALR1 and CU systems, varying the number of CPU cores (NCPU) used to multiples of the number of available cores on each compute node (Table I). In addition to this, two repeated simulations with 64 cores were done at ALR2–3 and once at the VC system, to generate simulations with 64 cores on all systems.

For simulations of the OBL, SIDE and FFR load cases with v10, two simulations were made on the VC system and one on the CU system, while three repeated simulations were made on the ALR1 system (Table I). For the SAFER HBM v9, all four load cases were repeated in a similar manner on the VC, ALR1 and CU system (Table I).

For most of the simulations the LS-DYNA default decomposition, i.e. the method to divide the model to each compute node and CPU, was used (Table I and Fig. A1 in the Appendix). To evaluate the influence of the decomposition on the numerical reproducibility, six additional simulations were run on the VC system with the LS-DYNA control card *CONTROL_MPP_DECOMPOSITION_TRANSFORMATION with option SX. This decomposition has been shown to be suitable for front crash simulations [15] and divides the model up into longitudinal slices compared with the patches of the default composition (Fig. A1 in the Appendix).

TABLE I

SIMULATION MATRIX WITH NUMBER OF CENTRAL PROCESSING UNIT CORES (NCPU) PER SIMULATION AND COMPUTER SYSTEM FOR EACH SIMULATION.

Loadcase	HBM Version	Decomposition	VC NCPU	ALR1 NCPU	ALR2 NCPU	ALR3 NCPU	CU NCPU
FF	v10	Default	(1–6)×28, 64	(1–4, 6–7)×32	64	64	(1–6)×32
	v10	Transformation: SX	(1–6)×28				
	v9	Default	120	16, 32, 128			64
OBL	v10	Default	64,120	32, 64, 128			64
	v9	Default	120	16, 32, 128			64
FFR	v10	Default	64,120	32, 64, 128			64
	v9	Default	120	16, 32, 128			64
SIDE	v10	Default	64,120	32, 64, 128			64
	v9	Default	120	16, 32, 128			64

A set of post-processing scripts which was implemented using Meta (Beta CAE Systems, Luzern, Switzerland) was used on all HPC systems to extract peak strain values, calculate injury criteria and risks. Some of the scripts used Matlab (Mathworks, Nattick, MA) for further processing of data extracted from the LS-DYNA binary databases by Meta (e.g. rib strain risk prediction). All processed data were saved in comma separated text-files and were further analyzed at the VC system. To analyze the variation in simulation responses of the six repeated FF simulations with the SAFER HBM v10, Shapiro-Wilk tests were used to assess normality of the analyzed data. Each sample was assessed for equal variances using an F-test, and lastly a one-way analysis of variance was carried out to assess if the mean values from each computer system were different. For the simulation responses analyzed, the Coefficient of Variation (CV) was calculated as the Standard Deviation (SD) divided by the mean. As the analysis of the FF load case showed that the variation of responses was randomly distributed and independent of the HPC system used, this was assumed also for the other load cases and their responses were pooled according to Table I for the CV calculation. All statistical analysis was carried out using Matlab and a significance level of 0.05 was used for all the tests. The v10 repeated simulations on the VC and ALR2–3 systems with the same NCPU (64) were not included in the averages analyzed.

III. RESULTS

Both the SAFER HBM v10 and v9 reached normal termination in all simulations, except for v10 which for an unknown reason did not start for NCPU=5×32 at the ALR1 system. In the normality check of the data from the six repeated simulations with the SAFER HBM v10 in the FF load case, four out of 66 measurements showed empirical evidence of not being normally distributed ($p<0.05$, Fig. 3–6). Six out of 66 did not have the same variance ($p<0.05$). Seven out of the 66 responses showed empirical evidence of having different means on different computer systems ($p<0.05$). The differences, although significant, were small in magnitude. Some of the calculated risks had a smaller CV than the injury criteria used for their prediction. This is an effect of saturation of the risk curve close to 100% risk caused by the high severity of the FF load case.

The global injury criteria evaluated, BrIC, HIC15, and anterio-posterior chestband deflection (Fig. 3), had a small CV (0.3–3.1%), and hence high reproducibility across the repeated simulations. All measurements had a normal distribution, equal variance, and equal mean at the 0.05 level.

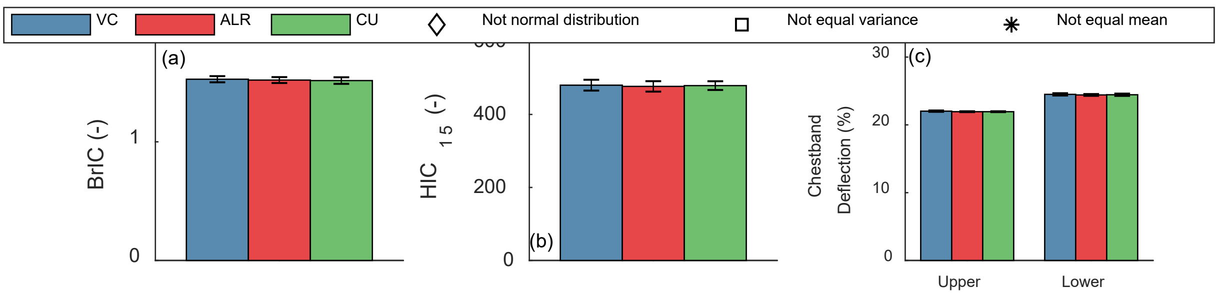

Fig. 3. Global injury criteria in the repeated FF simulations with the SAFER HBM v10 at each computer system.

The spinal cross-sectional forces and moments (Fig. 4) in the repeated FF simulations were highest at the L5 level, and for the L4 and L5 level both force and moment were normally distributed with equal variance and mean at the 0.05 level, while at L1–L3 means were different between computer systems.

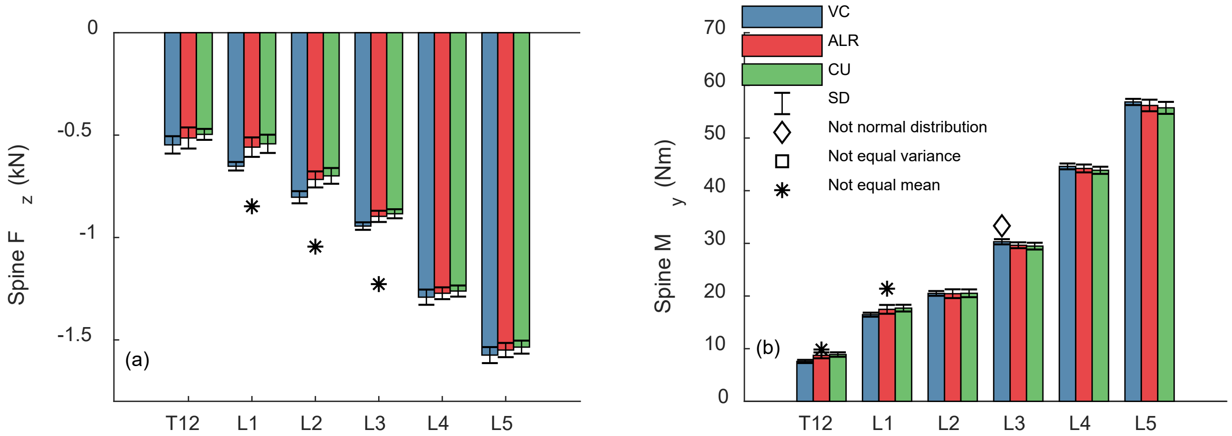

Fig. 4. Spinal cross-sectional forces (a) and flexion moment (b) for the 12th thoracic (T12) to 5th lumbar (L5) vertebra in the repeated FF simulations.

The KTH head model uses peak first principal Green strain as a tissue-based injury criterion to detect the risk of concussion. For the peak strain values extracted from the brain model, a trend toward higher mean peak values was seen on the VC system compared with the ALR and CU systems, but it was only the VC Gray Matter strain value and AIS 2 concussion risk, which could be differentiated from the ALR and CU simulations at the 0.05 level. The peak strain values were associated with a change of head rotational z-velocity, which occurred at 105 ms in the simulations as the head rebounded from a left rotation movement caused by the movement into the airbag, leading to a change of head z-rotational velocity of 115 rad/s over 45 ms (Fig. A3 in the Appendix).

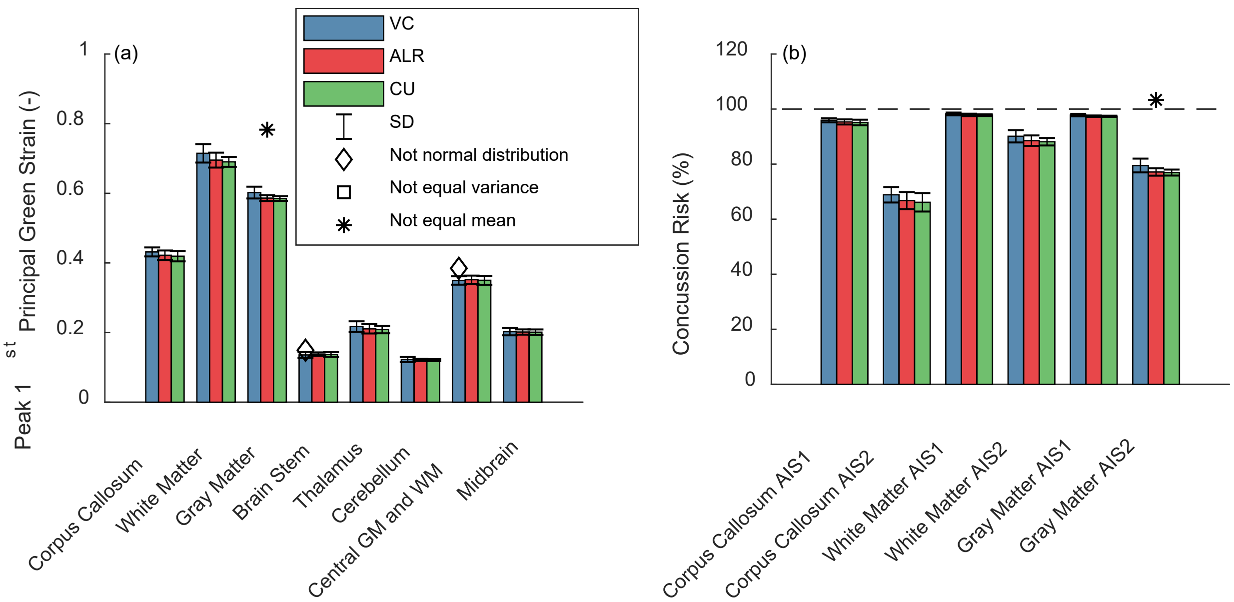

Fig. 5. (a) Peak first principal Green strain values for individual parts of the KTH brain model in the repeated FF simulations with the SAFER HBM v10 at each computer system. (b) Corresponding predicted Abbreviated Injury Scale (AIS) 1 and 2 concussion risks associated with the predicted strain values. SD = Standard Deviation.

Peak first principal strains in the middle layer of the rib cortical bone shells of up to 4.42% (SD 0.10%) were found in the repeated FF simulations (Fig. 6(a)), highest for the 4th left rib which was loaded by both seat belt and driver airbag at the time of the peak strain (Fig. A4 and Fig. A5 in the Appendix). The belt was directly above the left 3rd rib, which also experienced high strains at about 3.6%. Several of the rib fracture risk predictions (Fig. 6(b)), were close to 100%, and for the 75-year-old risk predictions no statistical analysis was done as all values were 100%.

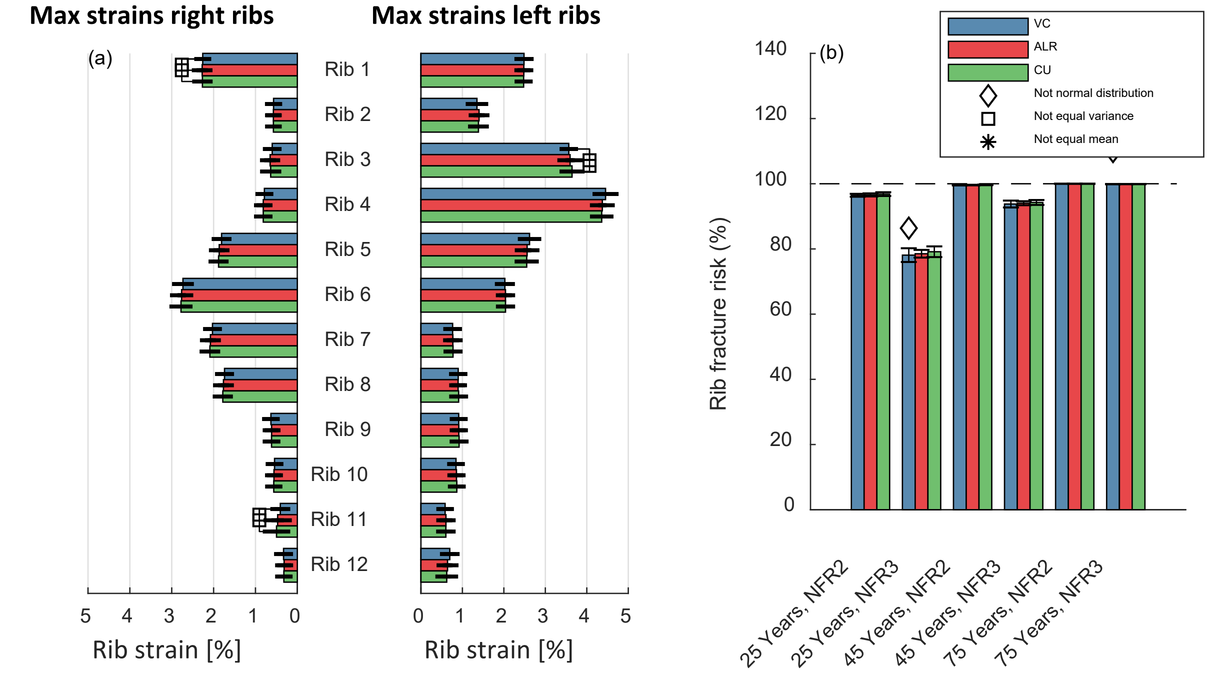

Fig. 6. (a) Peak maximum principal strain for each rib on the left and right side of the rib cage of the SAFER HBM v10 in the repeated FF simulations at each computer system. (b) Corresponding predicted rib fracture risk for two and three fractured ribs (NFR2 and NFR3) for occupants 25, 45, and 75 years of age.

The variation of HBM responses, as characterized by the CV of the measurements, varied in magnitude depending on the load case. It was smallest for the head values in side impact, with values below 1.9% for the updated SAFER HBM v10 (Table II).

TABLE II

COEFFICIENT OF VARIATION (CV) IN PERCENT FOR SELECTED HBM MODEL PREDICTIONS IN THE FULL FRONTAL (FF), NEAR-SIDE FRONTAL OBLIQUE (OBL), REAR SEAT FULL FRONTAL (FFR) AND SIDE IMPACT (SIDE) LOAD CASES.
VC, SX = SIMULATION WITH DECOMPOSITION TRANSFORMATION OPTION SX. N = NUMBER OF SIMULATIONS INCLUDED IN CALCULATION OF CV. SOLID GREEN INDICATES A VALUE CLOSE TO 0%, YELLOW 5% AND SOLID RED ABOVE 10% VARIATION. CHEST BAND DEFLECTIONS NOT AVAILABLE FOR THE V9 SIMULATIONS AND IN THE SIDE LOAD CASE.

Load case	HBM version	Computer system	n	Corpus callosum strain	White matter strain	Gray matter strain	BrIC	HIC15	Upper chest band	Lower chest band	L6	L7	L8	R6	R7	R8	L5 F_z
FF	v10	ALR1	6	3.3	3.1	1.4	1.6	3.0	0.3	0.5	2.0	5.7	2.5	3.2	2.9	3.3	2.2
FF	v10	CU	6	3.5	2.1	1.1	1.8	2.5	0.3	0.7	1.9	4.9	4.0	3.1	2.7	2.8	2.1
FF	v10	VC	6	3.0	3.7	2.8	1.7	3.1	0.4	0.7	2.4	4.4	3.3	2.6	1.7	2.1	2.5
FF	V10	VC, SX	6	3.1	3.0	2.3	1.5	4.9	1.3	1.0	1.9	5.6	4.3	2.1	2.1	4.1	3.8
FF	v9	All	5	0.9	2.6	1.2	1.6	0.6			1.5	5.5	1.9	2.2	1.2	1.2	0.9
OBL	v10	All	5	4.7	5.6	5.6	8.1	33.7	0.4	0.9	5.1	3.9	1.9	1.3	1.9	3.5	1.7
OBL	v9	All	5	12.5	11.4	8.9	4.7	10.2			7.0	4.1	25.6	4.7	5.7	7.7	1.8
FFR	v10	All	5	5.7	5.1	4.7	1.5	4.0	3.2	4.8	2.9	2.8	4.3	2.6	3.4	1.8	1.5
FFR	v9	All	5	5.5	5.4	6.9	1.8	6.7			3.3	5.1	4.3	2.4	1.7	1.6	1.3
SIDE	v10	All	5	0.9	1.4	1.9	0.6	1.3			7.5	2.6	4.6	1.6	1.9	3.1	20.2
SIDE	v9	All	5	1.0	1.4	0.8	0.7	0.7			0.7	1.1	1.8	2.6	6.7	0.8	0.9

In the OBL load case there were a number of measurements that had a CV of more than 10% for the v9, e.g. the peak brain strain values as well as the left 8th rib peak strain. Most of these were reduced for the v10 in the same load case, indicating an improvement in the numerical reproducibility. However, it should also be noted that the highest CV value found were for the HIC value in SAFER HBM v10 in the OBL load case. The head criteria for this load case was particularly spurious due to varying head impact conditions when the HBM slides off the driver airbag (Fig. 2(b)). For some simulations the HBM had a hard impact with its own left arm, the door trim or steering wheel rim, and for some this did not happen, causing the large variation in HIC value. For the same reason the BrIC value shows the highest CV in the OBL loadcase, while it was relatively stable with low variation in the other load cases (and more reproducible than the HIC value). Moreover, the L5 compressive (F_z) force in the side impact load case with the v10 model had a high CV, likely due to a low mean (−0.19 kN) leading to high CV with relatively small changes in the signal. Changing the model decomposition from the default to _TRANSFORMATION: SX did not have any influence on the response variation – some CV values were marginally reduced while others marginally increased. In addition, the SX option used 8–20% longer simulation time than the default decomposition. Furthermore, 5–10% shorter simulation times was obtained with the v10 compared with the v9 simulations on the VC systems for the same NCPU used.

For all the simulations with the SAFER HBM v10, which were repeated with 64 CPU cores at three different ALR systems, and at the VC and CU systems, the same result was obtained, down to four significant digits (Table AI in the Appendix). Some individual measurements deviate from this pattern, with some variations of the last two significant digits, for instance, HIC values on the ALR system for the FFR load case.

IV. Discussion

This study explored numerical reproducibility of local tissue-based (strain) and global injury criteria using the SAFER HBM in FE crash simulations. In the context of this study, numerical reproducibility means the ability of the FE simulation to produce the same results under varying simulation conditions. To investigate this repeated simulations were made with variation of the hardware and MPI software (by the use of five different HPC systems at three organizations), the decomposition of the model through simulations with different multiples of the NCPU on several compute nodes in the systems, and also by analyzing two different LS-DYNA model decomposition methods. Furthermore, the SAFER HBM was updated with a new pelvis, new subcutaneous soft tissue mesh and material models, contact definitions and global stiffness damping for the remaining elastic materials in the model. The last two actions were carried out particularly with the particular aim of improving the numerical reproducibility of the model. Simulations with both this updated SAFER HBM v10 and the previous v9 were made to allow for assessment of the effect of these updates.

Imperfect reproducibility, i.e. variation, in repeated testing with physical ATD models is well known and can easily be understood as the effect of manufacturing tolerances, the history of use of the ATD, inevitable variations in position and several other circumstances related to the testing procedure. For FE HBM simulations perfect repeatability is possible to achieve. In the work conducted for this study, repeated simulations on the same computer system with the same NCPU consistently gave the same results for all the load cases (however, these trivial results were omitted from the Results section). Perfect reproducibility of HBM crash simulation with LS-DYNA, was also shown to be possible on five different computer systems but conditioned to that the NCPU was held constant (Table AI). It is the decomposition of the model and the following variation of communication of information between the CPU that gives rise to a variation in the HBM response. The authors attribute most of this random variation in response, in the examples used in this study, to the contact interactions, illustrated by the largest variation of responses in the OBL load case in which the head of the HBM slides off the driver airbag and experiences varying head impact conditions depending on the NCPU used. Other explicit FE solvers used for crash-simulation which employ similar type of model decomposition and contacts are likely to exhibit similar variation in results with varying NCPU, but that remains to be verified by users of such codes in follow up studies.

To the best of our knowledge, even though consistency of distributed (MPP) LS-DYNA simulations has been studied previously [16], reproducibility of full-scale FE HBM crash simulations has not been studied in a similar way to the present study. Standardization of simulation procedures has been carried out, though: Klug *et al.* [17] developed a procedure for objective comparison of pedestrian FE HBM models using a generic passenger car front, standardized tracking of anatomical landmarks, posture, contact settings and post-processing. They found that small changes in initial posture, arm position, acetabulum height and head to acetabulum distance affected the head contact time. Additionally, contact algorithm and friction value affected the pedestrian kinematics and head contact time. This study resulted in the EuroNCAP Technical Bulletin 024 [18] which regulates the use of pedestrian HBMs to determine head contact timing and bonnet deflection due to body loading. The TB024 specifies that the solver version, platform, precision, NCPU and other settings should be the same between certification and application simulations. The findings of this study supports these requirements, but it is still likely that a sensitive HBM will give a different result between certification simulation and application simulation because as soon as the content of the overall FE model, consisting of HBM and vehicle model, changes the decomposition of the problem will also change, introducing the random variation found in this study.

The reproducibility of the updated SAFER HBM v10 and old v9 model was assessed by calculating the CV of a selected number of measurements (Table II). The most spurious load case was the OBL, in which the head of the occupant slides off the driver airbag towards the door trim, and the HIC value showed the highest CV value of all in the table for the v10 (and a range of HIC from 455 to 1028). At the same time, the CV for brain strain values was reduced from 9–13% for v9 to 5–6% for v10, most likely attributed to the update of the sliding contact of the brain skull interaction to a newer formulation. A similar trend towards reduced CV values in the OBL load case was seen for the selected rib strain values presented, from 4−26% variation in v9 reduced to 1.3−5% in v10.

Impact biomechanics testing and simulation with human surrogates, both HBMs and ATDs, ultimately tries to estimate risk of injury based on measured physical parameters. Such injury criteria are based on accelerations, forces and moments, deformation velocities or displacements for ATD, while for HBMs a higher specificity can be achieved by also studying the loading at tissue level in the form of strain-based injury criteria. The CV values calculated (Table II) showed that for the SAFER HBM v10 in the FF load case, the displacement based injury criteria (chest band compression) was the most reproducible with CV in the range of 0.3–1.3%, the velocity based BrIC second with 1.5–1.8%, followed by the lumbar F_z at 2.1–3.8%, brain strain at 1.1–3.7%, HIC at 2.5–4.9% and rib strain at 1.9–5.7%. NHTSA's [19] grading for ATD reproducibility classifies a CV below 5% as Excellent, and 5–8% as Good, but that would account for all types of random variation present in physical testing as outlined above, so the same grading cannot be applied to HBM results. The results from this study show that the SAFER HBM v10 has good reproducibility with some exceptions, such as the HIC value in the OBL load case. Special care should be taken for angled load cases with possible bifurcations of the contact problem, which can lead to large variations as found here. Otherwise, for the rib fracture prediction, which for a 25YO had a risk of 78.6% with a standard deviation of 1.65% for three rib fractures or more, for instance (Fig. 6(b)), the variation in responses seems acceptable for practical purposes such as optimizing a restraint system. The same variation in simulation response as found for the FE HBM here can be expected also for FE ATD models in full-scale crash simulations, but these will be less sensitive as most injury criteria used are kinematics and force based. With the CV values for HIC found for the HBM here, FE ATD models would have a reproducibility variation of the same magnitude as found for physical ATD [1].

The current approach with evaluation of HBM responses in repeated simulations with different NCPU could be employed in the validation or certification of HBMs to determine their sensitivity to differences in model decomposition. Two major contemporary FE HBMs [20–21] already incorporate the contact modelling techniques used in the present study to improve numerical reproducibility (large, generalized, single-surface segment-based contacts with damping and friction), but it is possible that there are other improvements to be made which would increase the confidence that a model's validated response in one setup is carried over to application setups. With respect to HBMs to be used for future proposed Virtual Testing, it will be of importance to quantify the sensitivity of a model to reproduce the same response with another decomposition, which is inevitable if the certification and application simulations are not identical and hence will be distributed differently to the processors used.

V. CONCLUSIONS

Numerically induced noise in FE HBM injury criteria responses was found to vary randomly with the number of CPUs used for simulation, but not due to different hardware or MPI software at each computer system used. Updates to the SAFER HBM reduced this variation in the near-side frontal oblique load case. For a fixed number of CPU cores, identical results were obtained from all computer systems. Thus, the main source of HBM response variation is the model decomposition. It is possible to quantify the numerical reproducibility of an HBM by repeated simulations varying the number of CPUs and analyzing the CV of the responses. The decomposition of an FE HBM will always vary between validation, certification and application simulation setup as a consequence of changing the model surrounding the HBM. Therefore, it is important to quantify the reproducibility of HBMs.

VI. ACKNOWLEDGEMENTS

This work was carried out at SAFER, Vehicle and Traffic Safety Centre at Chalmers University of Technology, Gothenburg, Sweden, and funded by FFI-Strategic Vehicle Research and Innovation, by Vinnova, the Swedish Energy Agency, the Swedish Transport Administration and the Swedish vehicle industry. Part of the simulations were performed on resources at Chalmers Centre for Computational Science and Engineering (C3SE) provided by the Swedish National Infrastructure for Computing (SNIC).

VII. REFERENCES

[1] Foster, J. K., Kortge, J. O., Wolanin, M. J. (1977) Hybrid III – A Biomechanically Based Crash Test Dummy. *Proceedings of the 21st Stapp Car Crash Conference*, SAE 770938. Warrendale, PA: Society of Automotive Engineers, pp.973–1014.

[2] Bortenschlager, K., Kramberger, D., *et al.* (2003) Comparison Tests of BioRID II and RID 2 with Regard to Repeatability, Reproducibility and Sensitivity for Assessment of Car Seat Protection Potential in Rear-End Impacts. *Stapp Car Crash Journal,* **47**: pp.470–488.

[3] Kazuki, H., Kazunori, M., Hidenori, M., Hiroyuki, M. (2017) Repeatability and Reproducibility of Upper Thorax Responses of THOR-50M ATDs. *Proceedings of the ESV Conference*, Detroit, MI, USA.

[4] van Ratingen, M. (2016) Bertil Aldman Memorial Lecture – Saving Lives with Safer Cars: The Past, Present and Future Consumer Safety Ratings. *Proceedings of the IRCOBI Conference*, Malaga, Spain.

[5] van Ratingen, M. (2020) Update on Virtual Testing in Safety Assessment of New Vehicles from Euro NCAP. *Presentation at the VIRTUAL-OSSCAR Workshop on Progress in Virtual Testing for Automotive Applications*.

[6] Schneider, L. W., Robbins, D. H., Pflüg, M. A., Snyder, R. G. (1983) *Development of anthropometrically based design specifications for an advanced adult anthropomorphic dummy family, Final Report*. University of Michigan Transportation Research Institute, Ann Arbor, MI.

[7] Pipkorn, B., Iraeus, J., *et al*. (2021) Validation of the SAFER Human Body Model Kinematics in Far-Side Impacts. *Proceedings of the IRCOBI Conference*, Munich, Germany.

[8] Kleiven, S. (2007) Predictors for Traumatic Brain Injuries Evaluated through Accident Reconstructions. *Stapp Car Crash Journal*, **51**.

[9] Iraeus, J., Pipkorn, B. (2019) Development and Validation of a Generic Finite Element Ribcage for Strain Based Fracture Prediction. *Proceedings of the IRCOBI Conference,* Florence, Italy.

[10] Östh, J., Bohman, K., Jakobsson, L. (2020) Evaluation of Kinematics and Restraint Interaction when Repositioning a Driver from a Reclined to an Upright Position Prior to Frontal Impact using Active Human Body Model Simulations. *Proceedings of the IRCOBI Conference*, Munich, Germany.

[11] Östh, J., Brolin, K., Bråse, D. (2015) A Human Body Model with Active Muscles for Simulation of Pretensioned Restraints in Autonomous Braking Interventions. *Traffic Injury Prevention*, **16**(3): pp.304–313.

[12] Ólafsdóttir, J. M., Östh, J., Brolin, K. (2019) Modelling Reflex Recruitment of Neck Muscles in a Finite Element Human Body Model for Simulating Omnidirectional Head Kinematics. *Proceedings of the IRCOBI Conference*, Florence, Italy.

[13] Pipkorn, B., Iraeus, J., Björklund, M., Bunketorp, O., Jakobsson, L. (2019) Multi-scale Validation of a Rib Fracture Prediction Method for Human Body Models. *Proceedings of the IRCOBI Conference*, Florence, Italy.

[14] Iraeus, J., Lindquist, M. (2016) Development and Validation of a Generic Finite Element Vehicle Buck Model for the Analysis of Driver Rib Fractures in Real Life Nearside Oblique Frontal Crashes. *Accident Analysis and Prevention,* **95**(Part A): pp.42–56.

[15] Kondo K (2012) Fujitsu's Activities in Improving Performance of LS-DYNA Nonlinear Finite Element Analysis Software. *Fujitsu Scientific and Technical Journal* 48(3): 375–383.

[16] Kan, C-D, Lin, Y-Y. (2000) Evaluation of Performance, Reliability and Consistency of MPP Version of LS-DYNA. *Proceedings of the International LS-DYNA Users Conference*, Detroit, MI, USA.

[17] Klug, C., Feist, F., *et al*. (2017) Development of a Procedure to Compare Kinematics of Human Body Models for Pedestrian Simulations. *Proceedings of the IRCOBI Conference*, Athens, Greece.

[18] Klug and Ellway (2019) Technical Bulletin TB 024 – Pedestrian Human Model Certification. Euro NCAP, Leuven, Belgium.

[19] NHTSA (2013) 49 CFR Part 572. Anthropomorphic Test Devices: Q3s 3-Year-Old Child Side Impact Test Dummy, Incorporation by Reference. *Federal Register* 78(225).

[20] Kato, D., Nakahira, Y., Atsumi, N., Iwamoto, M. (2018) Development of Human-Body Model THUMS Version 6 containing Muscle Controllers and Application of Injury Analysis in Frontal Collision after Brake Deceleration. *Proceedings of the IRCOBI Conference*, Athens, Greece.

[21] Schwartz, D., Guleyupoglu, B., Koya, B., Stitzel, J., Gayzik, F. S. (2015) Development of a Computationally Efficient Full Human Body Finite Element Model. *Traffic Injury Prevention,* **16**: S49–S56.

VIII. APPENDIX

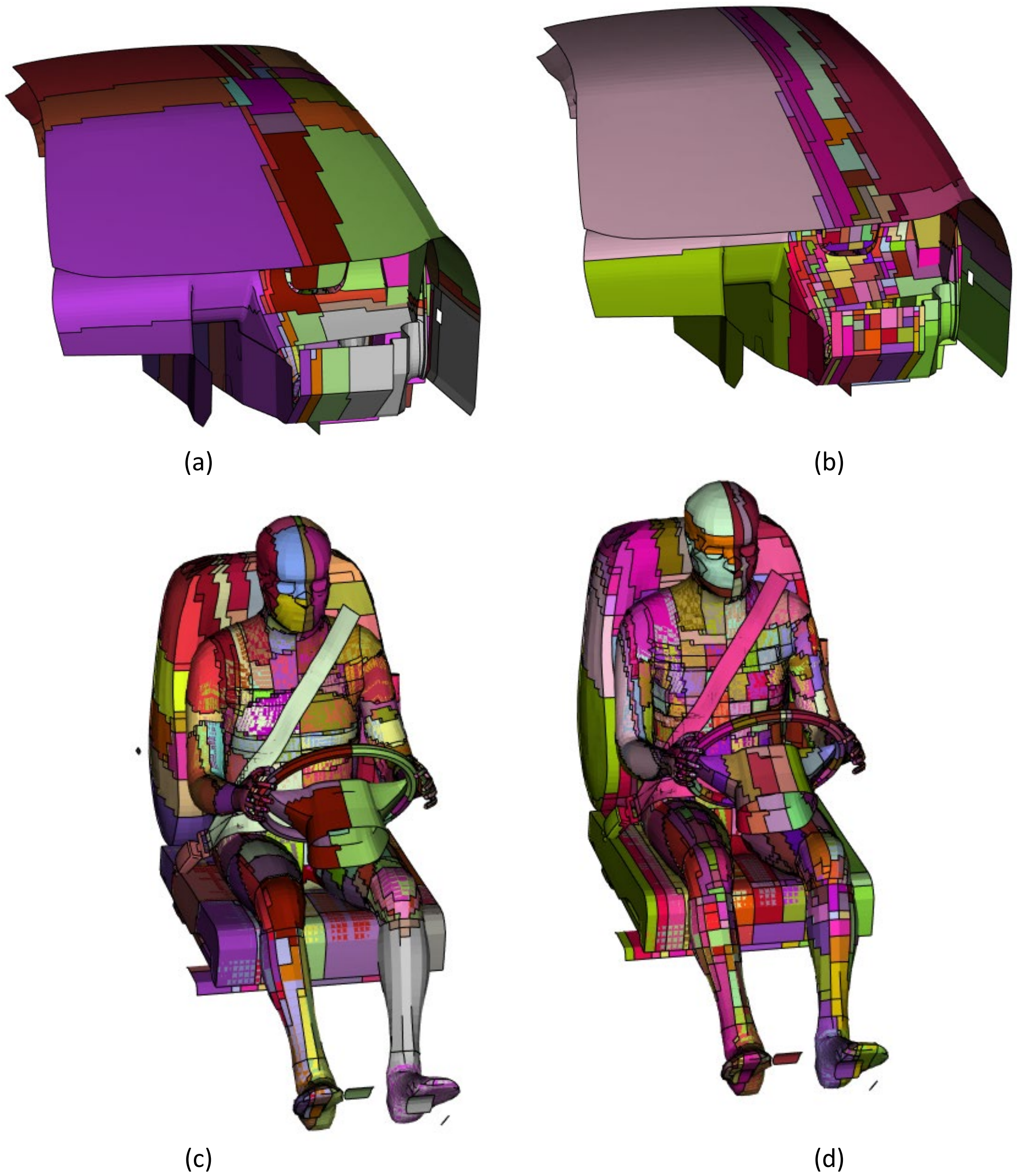

Fig. A1. Model overview showing the decomposition zones for a simulation on the VC system with NCPU = 112. Each colour represents the elements on one CPU core. (a) and (c): Default LS-DYNA decomposition. (b) and (d) Decomposition with *CONTROL_MPP_DECOMPOSITION_TRANSFORMATION with option SX.

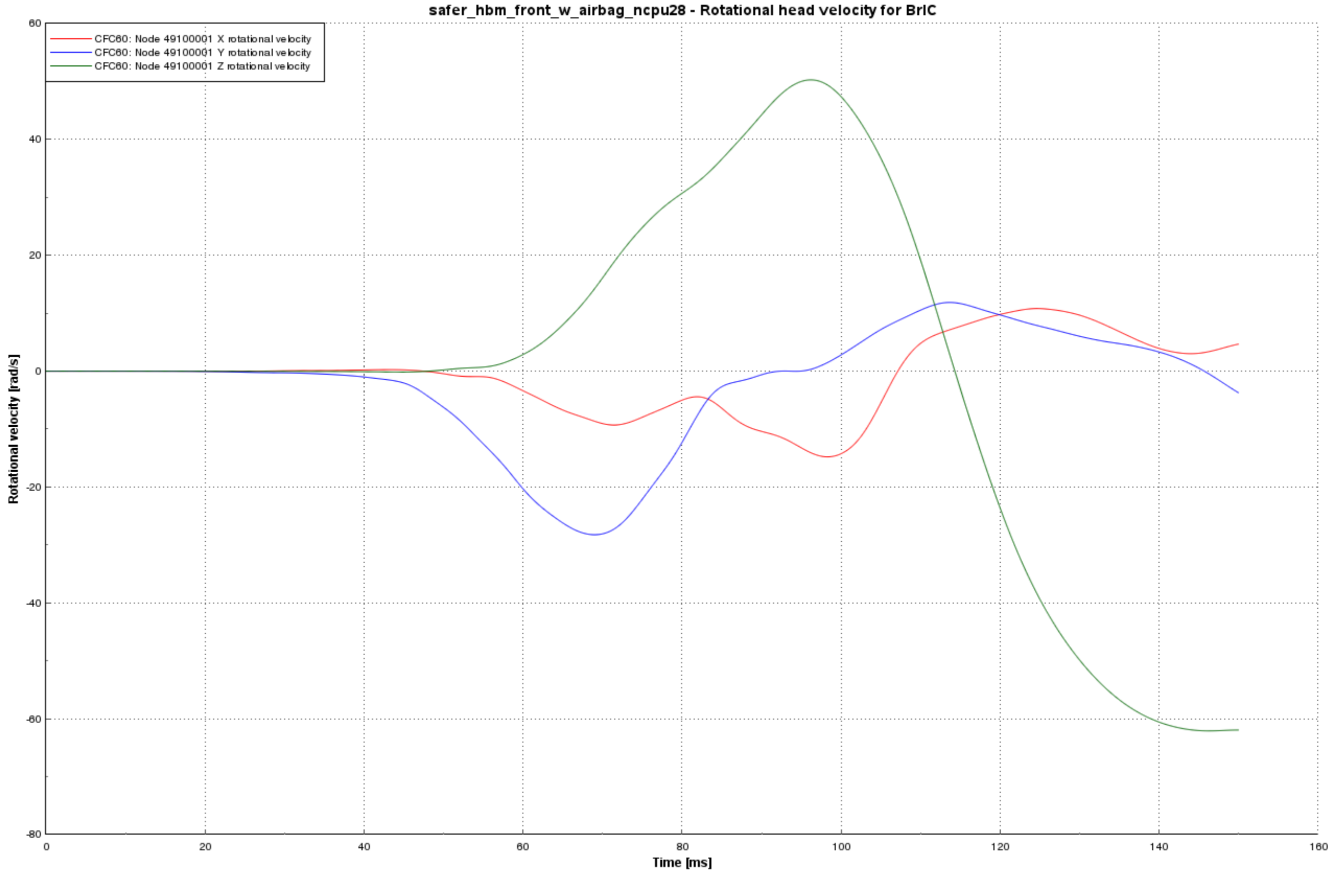

Fig. A2. Head rotational velocities in the FF load case with NCPU=28 on the VC system, filtered with a Channel Filter Class (CFC) 60 filter.

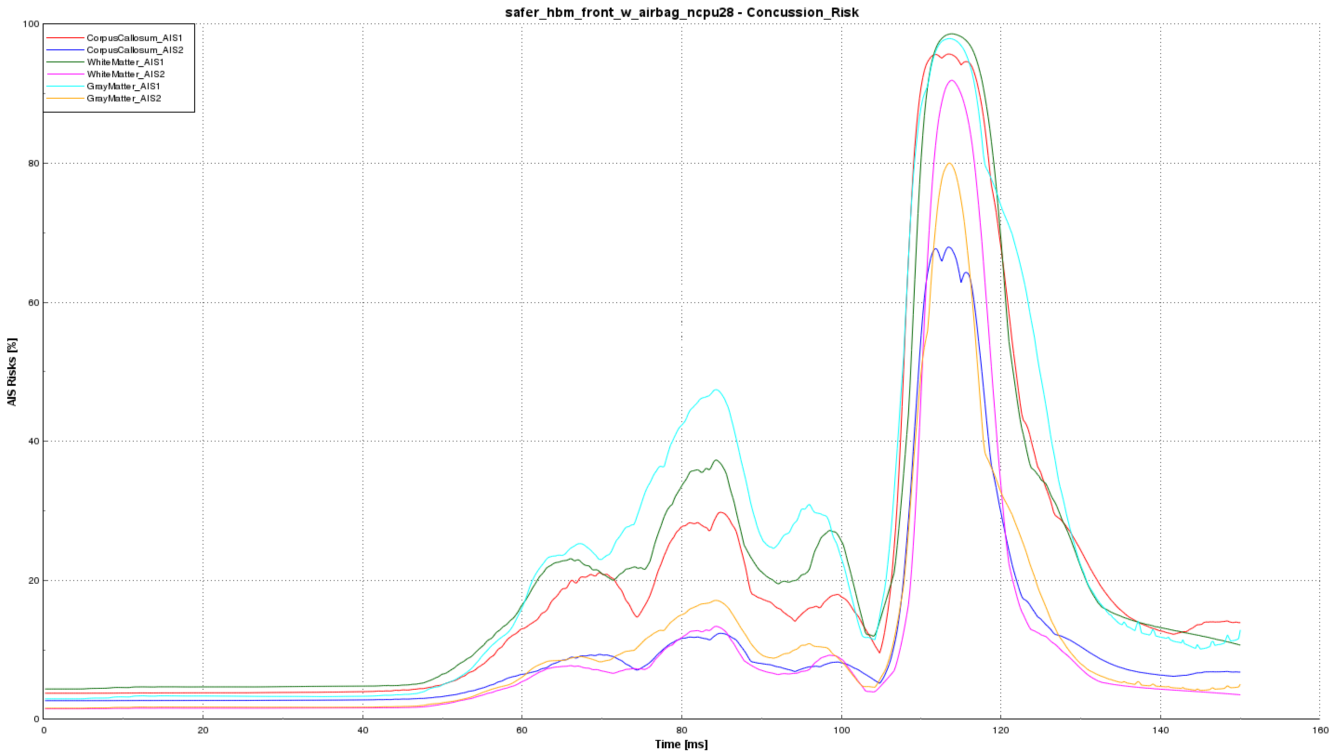

Fig. A3. Concussion risk curves in the FF load case with NCPU=28 on the VC system.

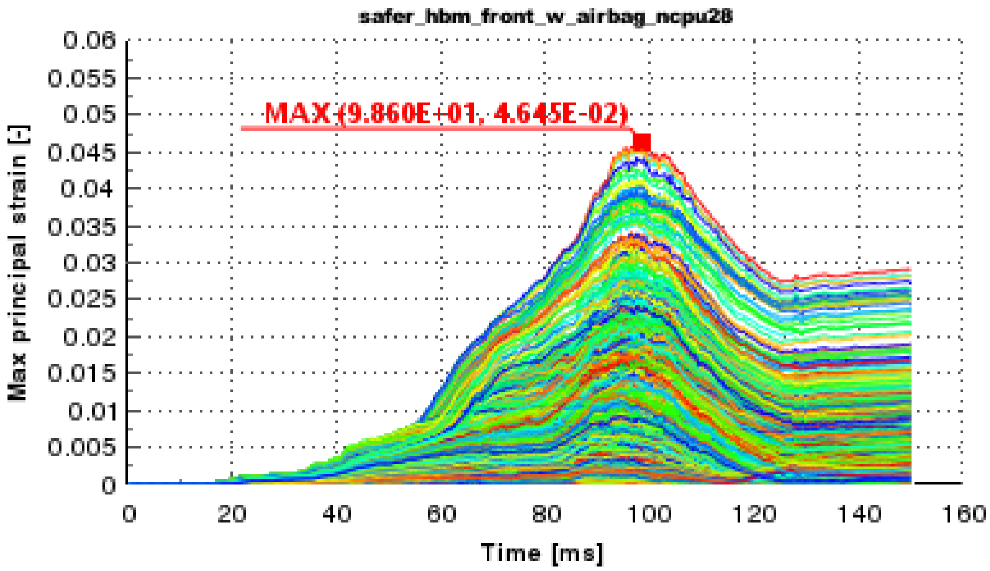

Fig. A4. Strain history for all elements of the 4th left rib in the FF load case with NCPU=28 on the VC system.

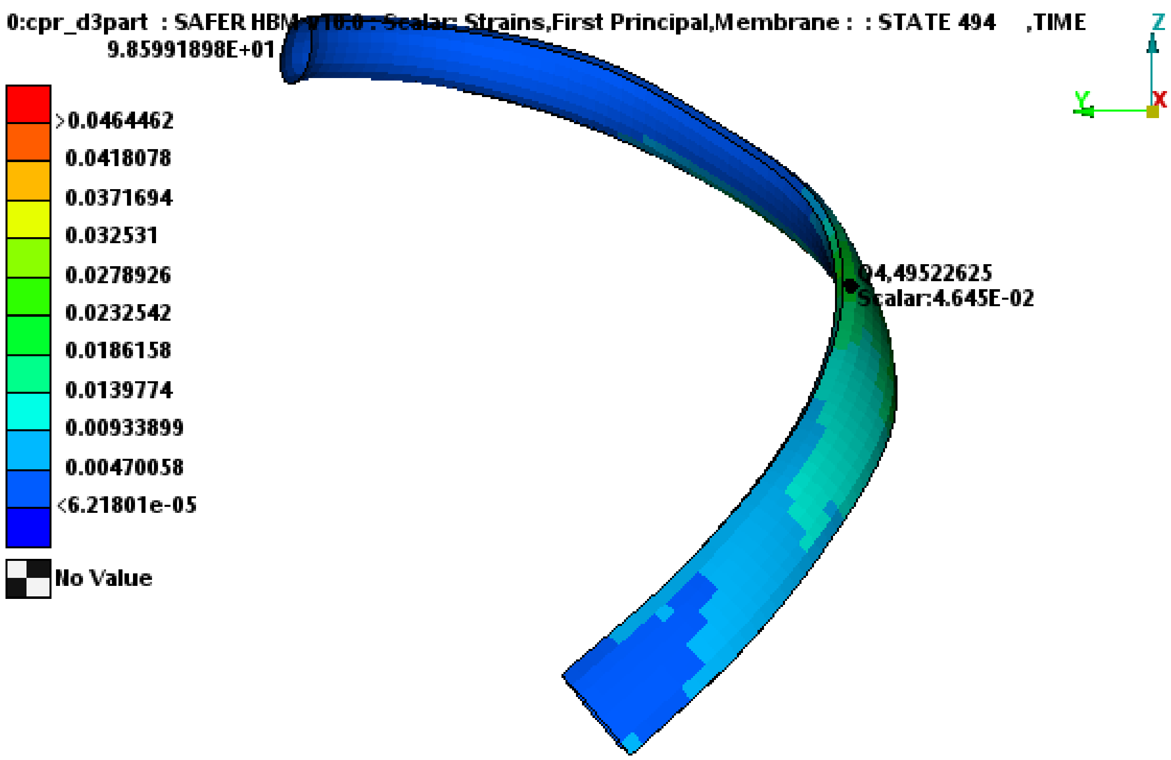

Fig. A5. Fringe plot of the 4th left rib in the FF load case with NCPU=28 on the VC system at the time with the highest peak max principal strain.

TABLE AI

RESULTING STRAIN VALUES AND GLOBAL CRITERIA VALUES FROM REPEATED SIMULATIONS WITH NCPU=64 FOR SAFER HBM V10 ON THE DIFFERENT COMPUTER SYSTEMS USED. DEVIATING VALUES INDICATED WITH BOLD TEXT.

Load case	HBM version	Computer system	Corpus callosum strain	White matter strain	Gray matter strain	BrIC	HIC15	Upper chest band	Lower chest band	L6	L7	L8	R6	R7	R8	L5 Fz
			(-)	(-)	(-)	(-)	(-)	(%)	(%)	(-)	(-)	(-)	(-)	(-)	(-)	(kN)
FF	v10	VC	0.4391	0.6952	0.5820	1.5300	474.0	**21.93**	24.33	0.0211	0.0080	0.0089	0.0279	0.0210	0.0184	-1.5200
FF	v10	ALR1	0.4391	0.6952	0.5820	1.5300	474.0	21.90	24.33	0.0211	0.0080	0.0089	0.0279	0.0210	0.0184	-1.5200
FF	v10	ALR2	0.4391	0.6952	0.5820	1.5300	474.0	21.90	24.33	0.0211	0.0080	0.0089	0.0279	0.0210	0.0184	-1.5200
FF	V10	ALR3	0.4391	0.6952	0.5820	1.5300	474.0	21.90	24.33	0.0211	0.0080	0.0089	0.0279	0.0210	0.0184	-1.5200
FF	v10	CU	0.4391	0.6952	0.5820	1.5300	474.0	21.90	24.33	0.0211	0.0080	0.0089	0.0279	0.0210	0.0184	-1.5200
OBL	v10	VC	0.6787	0.8114	0.8179	1.2710	739.0	**23.07**	**22.80**	0.0161	0.0172	0.0234	0.0226	0.0177	0.0131	-1.9290
OBL	v10	ALR1	0.6787	0.8114	0.8179	1.2710	739.0	23.08	22.78	0.0161	0.0172	0.0234	0.0226	0.0177	0.0131	-1.9290
OBL	v10	ALR2	0.6787	0.8114	0.8179	1.2710	739.0	23.08	22.78	0.0161	0.0172	0.0234	0.0226	0.0177	0.0131	-1.9290
OBL	V10	ALR3	0.6787	0.8114	0.8179	1.2710	739.0	23.08	22.78	0.0161	0.0172	0.0234	0.0226	0.0177	0.0131	-1.9290
OBL	v10	CU	0.6787	0.8114	0.8179	1.2710	739.0	23.08	22.78	0.0161	0.0172	0.0234	0.0226	0.0177	0.0131	-1.9290
FFR	v10	VC	0.1453	0.2555	0.2414	0.8500	714.0	**23.76**	**27.99**	0.0272	0.0158	0.0164	0.0347	0.0322	0.0343	-0.7330
FFR	v10	ALR1	0.1453	0.2555	0.2414	0.8500	**713.0**	23.78	28.00	0.0272	0.0158	0.0164	0.0347	0.0322	0.0343	-0.7330
FRR	v10	ALR2	0.1453	0.2555	0.2414	0.8500	**713.0**	23.78	28.00	0.0272	0.0158	0.0164	0.0347	0.0322	0.0343	-0.7330
FFR	V10	ALR3	0.1453	0.2555	0.2414	0.8500	**713.0**	23.78	28.00	0.0272	0.0158	0.0164	0.0347	0.0322	0.0343	-0.7330
FFR	v10	CU	0.1453	0.2555	0.2414	0.8500	714.0	23.78	28.00	0.0272	0.0158	0.0164	0.0347	0.0322	0.0343	-0.7330
SIDE	v10	VC	0.5963	0.9208	0.6805	0.8100	**222.0**	**6.42**	**2.87**	0.0242	0.0322	0.0299	0.0152	0.0103	0.0112	-0.1480
SIDE	v10	ALR1	0.5963	0.9208	0.6805	0.8100	221.0	6.40	2.90	0.0242	0.0322	0.0299	0.0152	0.0103	0.0112	-0.1480
SIDE	v10	ALR2	0.5963	0.9208	0.6805	0.8100	221.0	6.40	2.90	0.0242	0.0322	0.0299	0.0152	0.0103	0.0112	-0.1480
SIDE	V10	ALR3	0.5963	0.9208	0.6805	0.8100	221.0	6.40	2.90	0.0242	0.0322	0.0299	0.0152	0.0103	0.0112	-0.1480
SIDE	v10	CU	0.5963	0.9208	0.6805	0.8100	222.0	6.40	2.90	0.0242	0.0322	0.0299	0.0152	0.0103	0.0112	-0.1480